Plant Soil (2019) 439:339–355
https://doi.org/10.1007/s11104-019-04020-1

REGULAR ARTICLE

Differences in the relationship between metabolomic and ionomic traits of *Quercus variabilis* growing at contrasting geologic-phosphorus sites in subtropics

Huawei Ji · Vladimir Ossipov · Baoming Du · Jiahao Wen · Chunjiang Liu

Received: 18 August 2018 / Accepted: 28 February 2019 / Published online: 28 March 2019

Abstract

Aims Subtropical ecosystems are generally characterized by phosphorus (P)-deficient soils; however, extreme P-rich soils develop on phosphate rocks. We aimed to integrate metabolomic and ionomic analyses to survey how in situ trees adaptively respond to such contrasting P soils.

Methods Gas (GC-MS) or liquid (LC-MS) chromatography-mass spectrometry and inductively coupled plasma-optical emission spectrometer (ICP-OES) were used to analyze leaf metabolome and ionome of *Quercus variabilis*, which grew at two geologic P-rich and P-deficient sites in subtropical China.

Results Two *Q. variabilis* populations were significantly discriminated in terms of metabolome and ionome, with major contributions from 25 identified metabolites (e.g. sugars and P-containing compounds) and P and four other chemical elements. And of these 25 metabolites, orthophosphate was predominant in influencing the variation in the metabolomes of *Q. variabilis* between the two P-type sites. Moreover, orthophosphate was correlated with leaf P ($r = 0.85$, $p < 0.001$), while leaf P was significantly influenced only by soil resident P at the P-rich site. Furthermore, the metabolic pathway analysis indicated four critical metabolic pathways: galactose metabolism, amino sugar and nucleotide sugar metabolism, glyoxylate and dicarboxylate metabolism, fructose and mannose metabolism.

Conclusions These findings suggested that there were distinct ionome-metabolome interactions in *Q. variabilis* populations, between P-rich and P-deficient sites, which contributed to novel insights into how plants interactively adapt to P-limiting soils.

Keywords Ionome · Metabolome · Phosphate rocks · Soil nutrient variation · Adaptation · *Quercus variabilis*

Responsible Editor: John Hammond.

Electronic supplementary material The online version of this article (https://doi.org/10.1007/s11104-019-04020-1) contains supplementary material, which is available to authorized users.

H. Ji · B. Du · J. Wen · C. Liu (✉)
School of Agriculture and Biology and Research Centre for Low-Carbon Agriculture, Shanghai Jiao Tong University, Dongchuan Rd. 800, Shanghai 200240, China
e-mail: chjliu@sjtu.edu.cn

H. Ji · B. Du · J. Wen · C. Liu
Shanghai Urban Forest Research Station, State Forestry Administration, Beijing, China

V. Ossipov
Natural Chemistry Research Group, Department of Chemistry, University of Turku, Turku, Finland

V. Ossipov
Laboratory of Metabolomics, All-Russian Institute of Medicinal and Aromatic Plants, Moscow, Russia

C. Liu
Key Laboratory of Urban Agriculture, Ministry of Agriculture, Beijing, China

Introduction

Metabolomics is an important tool to study many ecological problems (Sardans et al. 2011a), including the

responses of plant metabolism to changes in the availability of mineral-nutrients (Fester et al. 2014; Hernández et al. 2007; Huang et al. 2008). Chemical elements contribute to the regulation of different physiological functions of plants; therefore, their availability may have a strong influence on the variation in the metabolome (Amtmann and Armengaud 2009; Hänsch and Mendel 2009; Soetan et al. 2010). Thus, the combination of metabolomics and the analysis of chemical elements can convey a more complete understanding of the adaptation and acclimation of plants to natural variation in soil nutrients (Guo et al. 2016; Ribeiro et al. 2016; Sanchez et al. 2011; Wu et al. 2013). However, to date, the effects of chemical elements on plant metabolism have been primarily investigated under controlled conditions, with a focus on only one or two nutrients (e.g., nitrogen (N) and phosphorus (P)) (Fester et al. 2014; Sardans et al. 2011a). Moreover, few studies involving combined metabolomic and ionomic responses to natural multi-nutrient variation have been conducted under long-term open field conditions (Wu et al. 2013).

Plant metabolome can be considered as the chemical phenotype of individual plants or maybe populations within a species (Rivas-Ubach et al. 2012), since their populations are geographically distinct or adapted to localized habitats (Davey et al. 2008). These populations may have unique metabolomes and ionomes when they are exposed to field conditions with contrasting nutrient content. This is particularly true for forest trees that have extended life spans (Brosché et al. 2005). For forest stands, the maximum heights of over-canopy trees are typically viewed as combined indicators of the site conditions, such as the supply of essential nutrients and soil moisture (Kimmins 2004). At forest sites, the status of essential nutrients within soils might serve as a major control for the growth of top trees in conjunction with their potential productivity (Cronan and Grigal 1995; Kimmins 2004; Koerselman and Meuleman 1996; Vitousek et al. 2010). Physiologically, the availability of nutrients in soils is associated with formation of several metabolites that positively or adversely influence the potential maximum growth of top trees within a stand (Rivas-Ubach et al. 2012). Moreover, the maximum growth rate capacity of organisms is characterized by a specific ratio of RNA to protein; and this ratio has been related to the organisms' N:P ratio (Irakli and Elser 2011). In the Mediterranean shrub *Erica multiflora*, for instance, increases in N:P ratio were accompanied by decreased proportions of primary metabolites (sugars, amino acids) relative to lipids and secondary metabolites, and also by lower growth rates (Rivas-Ubach et al. 2012).

Phosphorus comprises one of the primary life elements that is involved in a variety of biochemical processes, and is essential for the synthesis of many key compounds including nucleic acids, membrane lipids, etc. (Amtmann and Armengaud 2009; Westheimer 1987). Subtropical ecosystems are typically characterized as having P, calcium (Ca), and magnesium (Mg)-deficient soils, while they are enriched with iron (Fe) and aluminum (Al) due to strong weathering and leaching under high temperatures and moisture levels (Cleveland et al. 2011; Tiessen 2008; Walker and Syers 1976). This could result in the low P stoichiometry in plants (Han et al. 2005). Despite the low supply of P in soils, plant functionality may be maintained due to P conservation and utilization mechanisms in subtropical ecosystems (Attiwill and Adams 1993; Vitousek 1982). In terms of ecology, plants have evolved and formed ecotypic populations that are adapted to P-deficient habitats (Silberbush et al. 1981; Snaydon and Bradshaw 1962; Xiao et al. 2009; Yan et al. 1995). On the other hand, plants have developed dynamic strategies for coping with P-deficient soils in terms of morphology, physiology, biochemistry, mycorrhizal symbioses, etc. (Plaxton and Tran 2011; Sánchez-Calderón et al. 2010; Vance et al. 2003). For example, plants have evolved strategies, including modifications to root architecture and carbon metabolism and exudation of low molecular weight organic acids and enzymes, to obtain adequate P under limiting conditions (Shen et al. 2011; Vance et al. 2003). Moreover, plants can develop adaptive responses to utilize efficiently stored P by adjusting inorganic P (Pi) recycling internally, limiting P consumption, and reallocating P from old tissues to young growing tissues (Shen et al. 2011; Vance et al. 2003). Studies about the responses of plants to P deficiency is based mainly on experimental evidence obtained using the herbaceous model plant, *Arabidopsis thaliana*. However, it is unclear how woody plants adapt to natural P-deficient habitats in subtropical areas at the metabolomic level, which is closely related with the ionome in "soil-plant" systems (Gan et al. 2015).

In the Central Yunnan Plateau, which is located in subtropical China, some P-rich sites formed on P-rich ores (Yan et al. 2017), where soil resident P concentrations are six-fold higher (>1.2 mg g-1) than those at P-deficient sites. The content of other chemical elements, such as N, sulfur (S), Mg and Fe, are also significantly

higher (Ji et al. 2017; Tao 2005; Yan et al. 2011; Zhou et al. 2015). At these P-rich sites, there were significantly P-rich based stoichiometry in plants observed previously (Xiao et al. 2009; Zhou et al. 2015). Moreover, through the relative change of activities of metabolic pathways, plants could adapt to local environments with different soil P content (Raghothama 1999; Schachtman et al. 1998; Tillberg and Rowley 1989), and thus local phenotypes might be formed (Kawecki and Ebert 2004; Savolainen et al. 2007) and characterized based on their responses to different contents of soil nutrients (Shaver et al. 1979; Silberbush et al. 1981; Snaydon and Bradshaw 1962). This meant that there were several P-rich ecosystems distributed across P-limiting subtropics, which might have resulted in P-rich ecotype populations.

One Pan-Eastern-Asian distributed deciduous oak (*Quercus variabilis*) is a dominant tree species in the natural forest communities of the Central Yunnan Plateau, which possesses very high ecological, economic, and cultural importance (Chen et al. 2012). However, the distribution of *Q. variabilis* has greatly declined due to serious disturbances, such as cutting, grazing, and agricultural activity, which have left the stands highly fragmented. The renewal of forests in these areas requires an understanding of the relationships between tree growth and soil quality. For this study, we contrasted the leaf ionome (N, P, S, potassium (K), Ca, Mg, Fe, manganese (Mn), zinc (Zn), copper (Cu), and sodium (Na)) and metabolome of two *Q. variabilis* populations that were grown at a P-rich site and a P-deficient site. The question to be answered is what are the characteristic metabolites of in situ trees under such geologically-derived P-rich conditions in subtropical P-deficient zones. These results would be helpful toward elucidating how plants respond to increasing P in ecosystems due to anthropogenic activities.

Methods

Study sites

The study areas were located in the Central Yunnan Plateau, Yunnan Province, in Southwestern China. The P-rich site is situated on rocks that are rich in phosphate in Anning County, in close proximity to Kunming City (102°26′47.58″E, 24°58′54.38″N, 1869 m a.s.l.). The P-deficient site developed on non-phosphate rocks is situated in Mouding County, Chuxiong City (101°32′35.62″E, 25°14′48.25″N, 1846 m a.s.l.) (Ji et al. 2017; Zhou et al. 2015). The stands at both P-rich (Anning) and P-deficient (Chuxiong) sites are natural forests, which preserved up to the present time in spite on the irrational exploitation of the forest resources by the local population since the end of 1950 (Wu et al. 1987).

Table S1 displays the compositions and relative content (%) of the chemical elements of the phosphate rocks in Anning County (Tao 2005), and non-phosphate rocks (Matoushan Formation rocks) in Mouding County (Shi et al. 2011). Within this area, the primary soil groups are ferralosols and acrisols, according to WRB (FAO 1998). The chemical characteristics of the soils at the P-rich and P-deficient sites are shown in Table S2. The study area is subject to a plateau monsoon climate at low latitudes. In 2015, the climate conditions were similar between the two sites, with a mean annual temperature of 15.5 °C and mean annual precipitation of 897.5 mm. The mean monthly temperature and mean monthly precipitation of Anning and Mouding Counties from 1981 to 2010 are shown in Fig. S1. The growing season is approximately 250 days.

In the study areas, the vegetation is characterized as diverse; consisting of plants from tropical, subtropical, and temperate areas (Wu et al. 1987). Historically, this area was heavily forested; however, over the last 300 years, the natural forests were destroyed due to cutting, fires, grazing, and agricultural activities. The only natural forests remaining were left as fragmented patches, or located in remote mountainous areas. As a dominant species, *Q. variabilis* trees exist in small patches of pure stands, or as part of a mixture with other trees (e.g., *Q. acutissima, Q. aliena, Pinus* spp., *Picea* spp., etc.) (Wu et al. 1987).

Sampling

Within the mature *Q. variabilis* stands at each site, fifteen trees were randomly selected (distance from each tree was at least 20 m). The height and diameter at breast height (DBH) were measured for all selected trees at each site. In the stand at the P-rich site (Anning), the *Q. variabilis* trees ranged from 8.5 m to 23 m in height, and from 22.3 cm to 40 cm in DBH. In the stand at the P-deficient site (Chuxiong), the *Q. variabilis* trees ranged from 11 m to 16 m in height, and from 18.9 cm to 38.5 cm in DBH.

Soil and leaf samples for the analysis of chemical elements were collected in August 2015. Surface soil

cores (0–10 cm, 3 cm Ø) were collected from five places systematically arranged around of each selected tree at 1.5 m from the trunk. The collected samples were mixed to form a single composite soil sample for each tree. For the chemical analysis of the oak leaves, twenty of the youngest and most well-developed leaves were collected from each tree and dried at 60 °C for 48 h. For GC-MS and LC-MS analysis, five of the youngest and most well-developed leaves were collected from each tree and immediately frozen in situ in liquid nitrogen, and stored at −80 °C pending analysis. Thus, there were a total of 30 soil samples and 60 leaf samples.

Chemical analysis

For chemical analysis, all soil and leaf samples were digested with trace metal-grade nitric acid and diluted with distilled water. Total N concentration was analyzed with an elemental analysis-stable isotope-ratio mass spectrometer (Vario ELIII; Elementar, Germany). Total concentrations of P, S, K, Ca, Mg, Fe, Mn, Zn, Cu, and Na were analyzed using an inductively coupled plasma-optical emission spectrometer (ICP-OES) (Iris Advantage 1000; Thermo Jarrell Ash, Franklin, MA) (Sardans et al. 2011b; Sun et al. 2012). The concentrations of all elements were expressed as milligrams per gram of dry weight. All analyses were conducted at the Instrumental Analysis Centre of Shanghai Jiao Tong University.

GC-MS analysis of metabolites

Frozen leaves were lyophilized and ground to a fine powder using a ball-mill. The metabolites from the leaf samples were extracted according to (Lisec et al. 2006) with some modification. Samples of dry leaf powder (20 mg) were placed into 2-mL Eppendorf (EP) tubes to which 0.4 mL of extraction liquid (methanol-water, 3/1, *v*/v) was added. In addition, 20 μL of adonitol solution (2 mg mL^{-1} stock in dH2O) was added as an internal standard, and vortexed for 30 s. All of the samples were agitated via a ball-mill for 4 min. at 40 Hz, treated with ultrasound for 5 min. (incubated in ice water), and centrifuged for 15 min. at 13800×g at 4 °C. Supernatant solution (0.1 mL) from each sample tube was placed into a clean 2-mL glass vial for GC-MS analysis. Moreover, 10 μl from each extract was removed and pooled into a clean 2-mL glass vial as quality control (QC) sample. GC-MS analysis was composed of 30 samples and 7 QC samples.

The leaf extract samples were dried in a vacuum concentrator without heating, to which 80 μL methoxyamine hydrochloride (20 mg mL^{-1} in pyridine) was added, and incubated for 30 min. at 80 °C. Subsequently, 100 μL of N,O-Bis (trimethylsilyl)-trifluoroacetamide (BSTFA) reagent with 1% trimethylchlorosilane (TMCS, *v*/v) was added to the sample aliquots, incubated for 2 h at 70 °C, and cooled to room temperature. Moreover, 6 μL FAMEs (standard mixture of fatty acid methyl esters, C8-C16: 1 mg mL^{-1}; C18-C24: 0.5 mg mL^{-1} in chloroform) were added to the QC sample to facilitate the further calculation of the retention time index (RI) of metabolites, which was used for auxiliary qualitative analysis.

GC/TOFMS analysis was performed using an Agilent 7890 gas chromatography system coupled with a Pegasus HT time-of-flight mass spectrometer. This system utilized a DB-5MS capillary column coated with 5% diphenyl crosslinked with 95% dimethylpolysiloxane (30 m × 250 μm inner diameter, 0.25 μm film thickness; J&W Scientific, Folsom, CA, USA). A 1 μL aliquot of the analyte was injected in splitless mode. Helium was used as the carrier gas, the front inlet purge flow was 3 mL min^{-1}, and the gas flow rate through the column was 1 mL min^{-1}. The initial temperature was kept at 80 °C for 1 min., which was then raised to 290 °C at a rate of 10 °C min^{-1}, and kept at 290 °C for 12 min.. The injector, transfer line, and ion source temperatures were 280, 270, and 220 °C, respectively. The energy was −70 eV in electron ionization mode. Mass spectrometry data were acquired in full-scan mode with the m/z range of 50–600 at a rate of 20 spectra per second after a solvent delay of 8.1 min..

LC-MS analysis of metabolites

For UHPLC-QTOF-MS analysis, metabolites from samples of dry leaf powder were extracted according to (De Vos et al. 2007) with some modification. 50 mg samples in 2 mL EP tubes were homogenized employing a ball mill (40 Hz, 5 min.) after adding two steel balls, 200 μL H_2O and 800 μL MeOH:ACN (1:1, *v*/v). The samples were subsequently incubated for 1 h at −20 °C, followed by 15 min. Centrifugation at 13800×g at 4 °C. A supernatant solution (800 μL) from each resulting extract was obtained and evaporated to dryness in a vacuum concentrator. The dry extracts were then re-dissolved in 100 μL of ACN:water (1:1, *v*/v), vortexed for 30 s and then sonicated for 10 min. in a water bath at 4 °C. The extracts were then centrifuged 15 min. at

13800×g at 4 °C, whereafter 10 μL of supernatant solution from each tube was pooled together as a QC sample. Extract derived supernatant solutions of 70 μL were used for UHPLC-QTOF-MS analysis.

UHPLC-QTOF-MS analysis was performed using an Agilent 1290 UHPLC system (Agilent Technologies) with a UPLC BEH Amide column (1.7 μm, 2.1 × 100 mm, Waters) coupled to a TripleTOF 6600 (Q-TOF, AB Sciex). The mobile phase consisted of water (including 25 mM NH_4OAc and 25 mM NH_4OH) (pH = 9.75) (A) and acetonitrile (B). The elution profile was as follows: 0–1 min., 85% B (15% A) (isocratic); 1–12 min., 85–65% B (15–35% A) (linear gradient); 12–12.1 min., 65–40% B (35–60% A) (linear gradient); 12.1–15 min., 40% B (60% A) (isocratic); 15–15.1 min., 40–85% B (60–15% A) (linear gradient); 15.1–20 min., 85% B (15% A) (isocratic). The flow rate was 0.3 mL min^{-1} and the sample injection volume was 2 μL. The analysis time was 20 min..

The TripleTOF mass spectrometer was used for its ability to acquire MS/MS spectra on an information-dependent basis (IDA) during the LC-MS experiments. In this mode, the acquisition software (Analyst TF 1.7, AB Sciex) continuously evaluates the full scan survey MS data as it collects and triggers the acquisition of MS/MS spectra depending on preselected criteria. In each cycle, 6 precursor ions whose intensity greater than 100 were chosen for fragmentation at collision energy (CE) of 35 V (15 MS/MS events with product ion accumulation time of 50 msec each). The ESI source conditions were set as follows: ion source gas 1, 60; ion source gas 2, 60; curtain gas, 30; source temperature, 550 °C and Ion Spray Voltage Floating (ISVF), 5500 V or − 4500 V in positive or negative modes, respectively. To assess the column condition and data quality, the QC sample was analyzed six times during the all sequence of UHPLC-MS analysis.

Data processing for GC-MS analysis

For GC-MS analysis, the Chroma TOF 4.3X software of LECO Corporation and LECO-Fiehn Rtx5 database were applied for raw data extraction, baseline filtering and calibration, peak alignment, deconvolution of mass-spectra, peak area integration, and metabolite identification (Kind et al. 2009). Discriminating compounds were identified by matching their similarity and RI values with data from the LECO/Fiehn Metabolomics Library. Peaks with mass-spectrum similarity greater than 800 (full similarity is 1000) and RI difference less than 5000 were reliably identified. Two discriminating compounds were identified putatively because their RI difference was less 5000, but the mass-spectrum similarity was only about 635–637. A total of 438 peaks were detected in the leaf samples. The missing values in a table of raw data were filled up by half of the minimum value. The relative content of metabolites was calculated by normalizing their peak areas to the response of internal standards**.** The resulting three-dimensional data, which included the sample name, peak number, and normalized peak area were used for statistical analyses.

Data processing for LC-MS analysis

Raw LC/MS data were processed using XCMS software for peak detection, chromatogram alignment, and peak identification (Smith et al. 2006). The identifications were completed by matching the acquired MS/MS data, assembled in in-house developed database. A total of 24,421 and 29,926 mass peaks in the leaf samples were detected in positive and negative modes, respectively, where 2205 and 2806 metabolites could be left, respectively, through a RSD < 30% denoising method (the peak of RSD < 30% was kept in the QC sample) and then filling up the missing values of raw data by half of the minimum value. In addition, an overall normalization method was employed in this data analysis. Subsequently, the resulting three-dimensional data in positive or negative modes, which involved the sample name, peak number, and normalized peak area were utilized for statistical analyses.

Statistical analyses

Four resulting matrixes of ionomic and metabolomic data (GC-MS, UPLC-MS positive mode and UPLC-MS negative mode) were exported into SIMCA-P+ software package (version 13, Umetrics, Umeå, Sweden), log-transformed to improve normality and used for multivariate data analysis. At the first step, principal component analysis (PCA) was applied to reveal the homogeneity of the data, any groupings, trends and outliers. Outliers were found with application of the Hotelling's T2 ellipse (95% confidence interval) and by the distance to model parameter (DModX) that based on the model residuals and shows the distance to the model plane for each observation. All outliers were carefully examined and if they enhance strong within group variation and significantly

disturb the PCA model, removed from the dataset. Further, in order to specify the metabolic and ionomic differences between samples from P-rich and P-deficient sites, data were Pareto-scaled and analyzed using a supervised classification method – orthogonal partial least-squares to latent structures discriminant analysis (OPLS-DA) that separates predictive variation (between groups) from nonpredictive variation (within groups) (Fonville et al. 2010).

Seven-fold cross validation was employed to estimate the robustness and the predictive ability of the supervised OPLS-DA, whereas for the significance testing of the OPLS-DA models, ANOVA of the cross-validated residuals (CV-ANOVA) or a permutation test was applied. In addition, an R^2 value of >0.7 and an Q^2 value of >0.4 denoted a highly significant model (Lundstedt et al. 1998). Based on OPLS-DA, a loading plot was constructed, and the first principal component of variable importance projection (VIP) was obtained. In order to select metabolites or chemical elements that had the strongest and most significant effects on the discrimination of oak trees from P-rich and P-deficient experimental sites, VIP values that exceeded 1.0 and Student's *t* test ($p < 0.05$) between two comparison groups were applied. Subsequently, Pearson's correlation analysis was calculated for samples from P-rich or P-deficient sites to demonstrate the relationships between the content of the identified and discriminating metabolites and the content of the discriminating elements that were obtained from the OPLS-DA analyses. The correlation analyses were carried out with SPSS 18.0 (SPSS Inc., USA).

Weight analysis of metabolic pathways of *Q. variabilis* between P-rich site and P-deficient site was performed with the application of MetaboAnalyst 3.0 (MetPA) (http://metaboanalyst.ca/) based on all identified and discriminating metabolites obtained from the OPLS-DA analysis. The pathway impact value (pathway impact, PI) calculated from pathway topology analysis and enrichment analysis was used to evaluate the weight of the metabolic pathway in the whole metabolic regulatory network, and the pathway impact value threshold was set at 0.1(Xia et al. 2015; Xia and Wishart 2010).

Results

The quantification of chemical elements in the leaves of *Q. variabilis* trees that grew at the two experimental sites with high (P-rich site) and low (P-deficient site) soil phosphorus content exhibited significant differences in the content of other chemical elements: N, S, K, Mg, Fe, Mn, Zn, and Cu (Table 1). Based on the principal component analysis (PCA) of leaf ionomic data, two *Q. variabilis* populations from the P-rich and P-deficient sites were clearly distinguished by the first principal component (PC1), which represented 43.9% of the variation (Fig. 1a). The same pattern was found with the analysis of metabolomic data that was obtained from LC-MS analysis, in both negative and positive modes, where the two populations of *Q. variabilis* trees were separated by their first principal components (PC1), which both represented 11% of the variation (Fig. 1b and c). However, based on the PCA of leaf metabolomic data obtained from GC-MS analysis, metabolite composition of *Q. variabilis* did not clearly differ between the two tree populations from the P-rich and P-deficient sites (Fig. 1d).

Following the removal of outliers, the OPLS-DA analysis of ionomic data and metabolomic data, obtained from both LC-MS and GC-MS analysis, all showed that the population of *Q. variabilis* trees at the P-rich site significantly differed from those at the P-deficient site (Fig. 2a, b, c, and d). CV-ANOVA data and cross-validation plots revealed that the differences between models were statistically significant and reliable (Fig. S2). Loading plot data of the first latent variable and VIP > 1 values were applied for the selection of the potential markers that discriminated the two populations of *Q. variabilis* trees (Table 2). As a result, it was determined that the strongest discriminating powers had 25 identified metabolites, P, and four other chemical elements (N, S, Fe, and Zn) (Table 2, Tables S3 and S4). The content of all element-markers and 21 metabolite-markers were higher in the leaves at the P-rich site than those at the P-deficient site, with the exceptions being D-allose, stachyose, L-malic acid, and betaine. Among all of the metabolites, orthophosphate showed a high contribution (VIP value = 2.63) toward the discrimination of the two *Q. variabilis* populations.

Moreover, when all metabolite data obtained from LC-QTOF-MS in negative and in positive modes and GC-MS were using together for PCA and OPLS-DA analysis, two *Q. variabilis* populations from P-rich and P-deficient sites were clearly separated (Fig. S3a), and among all the metabolites, orthophosphate showed the highest contribution (VIP value = 2.3) in discriminating the two *Q. variabilis* populations (Fig. S3b and Fig. S3c).

Table 1 Content of chemical elements in soils and leaves of oak trees at P-rich and P-deficient sites (mg g^{-1}). Significance of differences in the element concentrations between two sites: * $p < 0.05$, ** $p < 0.01$ and *** $p < 0.001$; n.s. – not significant

Element	Soils					Leaves				
	P-rich site		P-deficient site		*p* value	P-rich site		P-deficient site		*p* value
	Mean	CV, %	Mean	CV, %		Mean	CV, %	Mean	CV, %	
N	1.31	22.5	0.99	26.5	**	18.85	7.7	16.29	11.2	***
P	6.53	134.4	0.25	22.4	*	2.16	32.6	1.16	16.1	***
S	0.37	47.6	0.16	20.7	***	1.96	15.8	1.27	10.1	***
K	11.41	29.0	7.16	56.7	**	5.59	13.4	4.79	13.9	**
Ca	7.76	205.0	0.54	62.7	n.s.	8.04	15.6	8.25	21.5	n.s.
Mg	3.31	16.7	2.25	48.1	**	1.74	24.4	1.40	25.5	*
Fe	43.75	32.7	26.46	42.2	**	0.26	16.5	0.13	16.5	***
Mn	0.64	46.3	0.28	56.4	***	2.12	27.6	2.50	34.8	n.s.
Zn	0.20	26.5	0.11	148.5	*	0.10	15.7	0.02	25.9	***
Cu	0.06	30.0	0.03	42.6	***	0.01	52.7	0.01	53.7	n.s.
Na	1.22	81.2	0.67	35.2	n.s.	0.75	125.2	0.38	65.8	n.s.

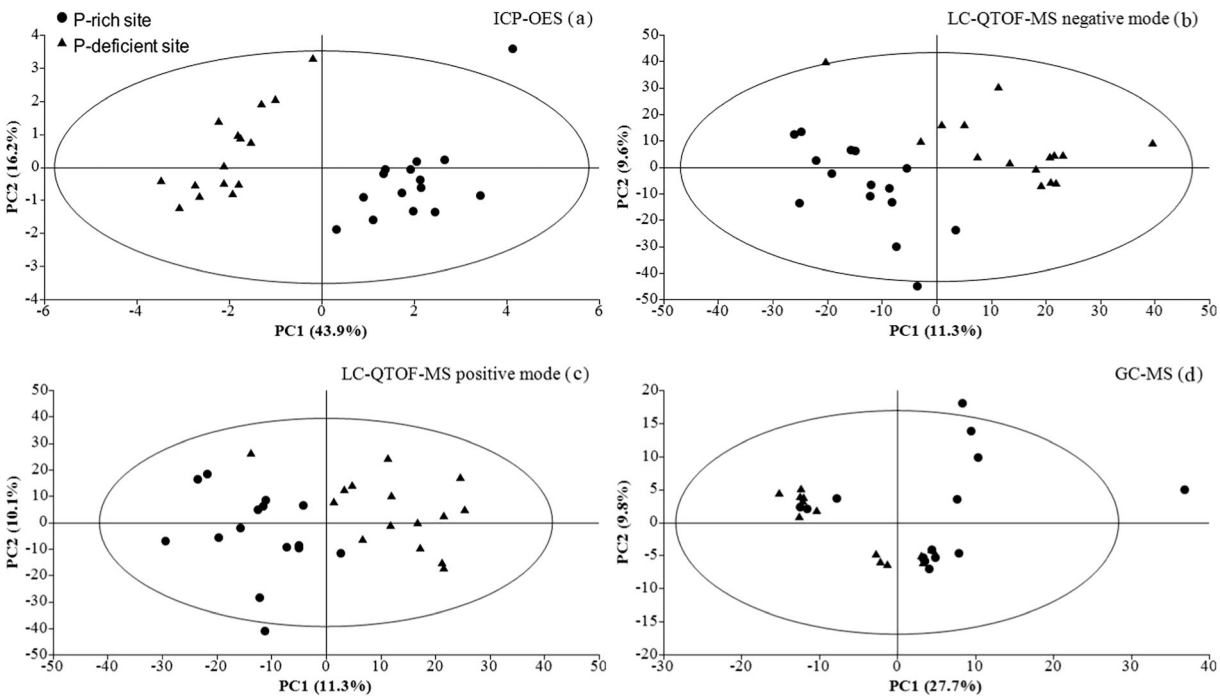

Fig. 1 Score plots of principal component analysis (PCA) of ionomic (**a**) and metabolomic (**b**-**d**) data obtained for leaf samples of *Q. variabilis* trees growing at P-rich (circles) and P-deficient (triangles) sites. (**b**) LC-QTOF-MS in negative mode (2806 variables), (**c**) LC-QTOF-MS in positive mode (2205 variables) and (**d**) GC-MS (421 variables). PC1 and PC2 are the first and the second principal components. Outliers determined with application of the Hotelling's T2 ellipse (95% confidence interval) and by the distance to model parameter (DModX) were evaluated and removed from datasets. To find out ionomic and metabolomic markers that discriminated leaf samples of *Q. variabilis* trees from the two experimental sites, the four processed datasets were analyzed with a supervised classification method (OPLS-DA) (see Fig. 2)

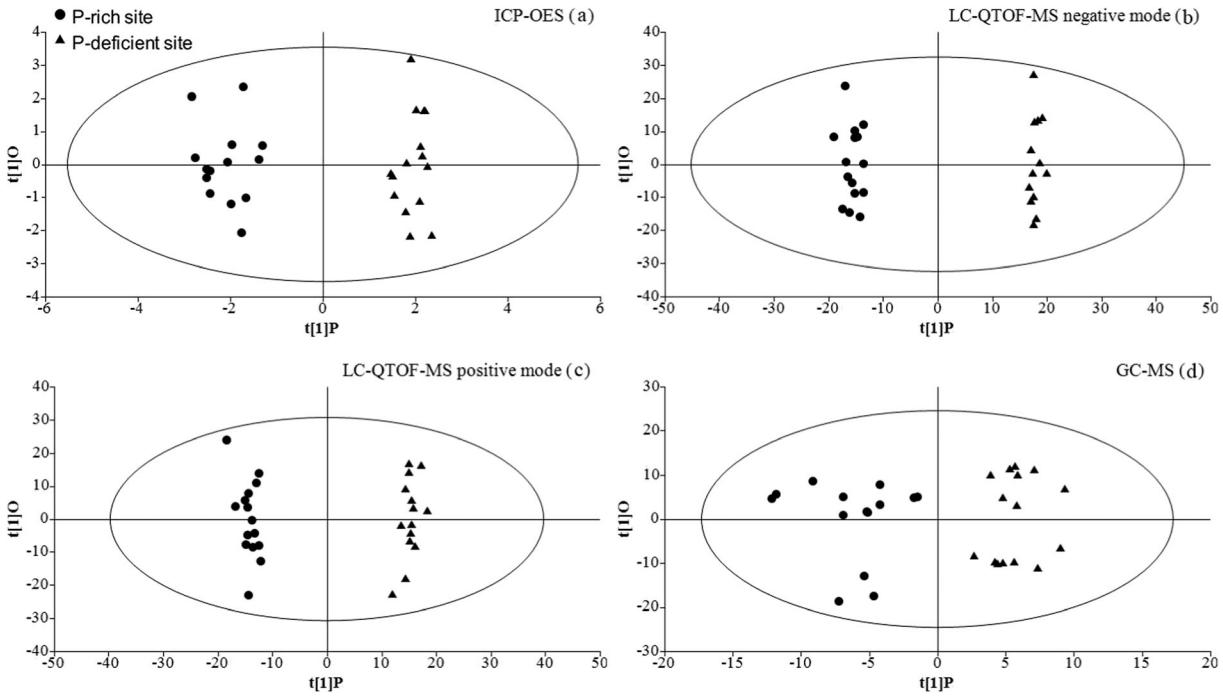

Fig. 2 Score plots of orthogonal projections to latent structures discriminant analysis (OPLS-DA) of ionomic (**a**) and metabolomic (**b-d**) datasets obtained for leaf samples of *Q. variabilis* trees growing at P-rich (circles) and P-deficient (triangles) sites. Evaluation of four obtained OPLS-DA models (**a-d**) showed high and significant separation of leaf samples of *Q. variabilis* trees from the two experimental sites with the first predictive component (t[1]P): (**a**) ionomic dataset ($R^2Y[1] = 0.97$, $Q^2[1] = 0.95$, CV-ANOVA $p < 0.0001$), (**b**) LC-QTOF-MS in negative mode ($R^2Y[1] = 0.99$, $Q^2[1] = 0.83$, CV-ANOVA $p < 0.0001$), (**c**) LC-QTOF-MS in positive mode ($R^2Y[1] = 0.99$, $Q^2[1] = 0.77$, CV-ANOVA $p < 0.0001$) and (**d**) GC-MS ($R^2Y[1] = 0.85$, $Q^2[1] = 0.49$, CV-ANOVA $p < 0.01$)

In order to find metabolic pathways related to differences between the two P-type sites, we used weight analysis to analyze the metabolic pathways of *Q. variabilis* related to 25 identified and discriminating metabolites (Table 2). The *p* value was calculated from the enrichment analysis and the PI value was calculated from the pathway topology analysis. With the application of MetPA, we identified six pathways with PI ≥0.1, however, there were only four pathways with both PI ≥0.1 and $p < 0.05$: galactose, amino sugar and nucleotide sugar, glyoxylate and dicarboxylate, and fructose and mannose (Fig. 3 and Table S5), which were the most relevant pathways differentially regulated in the leaves of the two *Q. variabilis* tree populations at the P-rich and P-deficient sites (Fig. 3). The highest weight was found for the amino sugar and nucleotide sugar pathway (PI = 0.25) that involved five metabolites (UDP-D-galactose, UDP-D-glucose, UDP-N-acetylglucosamine, D-mannose, and D-mannose-1-phosphate (Table S5). A metabolic network was constructed in a framework that reflected the four major pathways (Fig. 4).

Correlation analysis revealed that the concentrations of leaf total P were positively associated with orthophosphate content in *Q. variabilis* leaves, at both the P-rich and P-deficient sites (Table 3). Moreover, at the P-rich site, there were positive relationships between leaf N, D-proline, and γ-aminobutyric acid; leaf total P, D-mannose, D-mannose-1-phosphate, and UDP-N-acetylglucosamine; leaf S and ethanolamine; leaf Fe and 4-hydroxycinnamic acid; and leaf Zn and 2-hydroxypyridine. Further to this, there were negative relationships between leaf N and succinic acid; leaf S and L-malic acid; and leaf Fe, D-mannose 1-phosphate, ethanolamine, glycerol, and orthophosphate (Table 3).

At the P-deficient site, there were positive relationships between leaf N, D-mannose, D-proline, and pyruvaldehyde; and leaf Zn and ethanolamine. Moreover, there were negative relationships between leaf N, betaine, and UDP-N-acetyl-glucosamine; leaf total P and glycerol; leaf S and 4-hydroxycinnamic acid; and leaf Fe, 1,5-anhydroglucitol, anabasine, D-talose, glycolic acid (Table 3).

Table 2 Chemical elements and metabolites responsible for discrimination of *Q. variabilis* trees growing at the P-rich and P-deficient sites that were selected from four OPLS-DA models on the basis of VIP > 1 and *t*-test ($p < 0.05$) values

ID	Name	Classification	Relative content		Fold change	*p* value	VIP
			P-rich site	P-deficient site	Log (P-rich site/P-deficient site)		
	N	Chemical elements	18.979	16.287	0.066	0.000	1.042
	P	Chemical elements	2.199	1.160	0.278	0.000	1.320
	S	Chemical elements	1.901	1.271	0.175	0.000	1.427
	Fe	Chemical elements	0.263	0.132	0.298	0.000	1.456
	Zn	Chemical elements	0.056	0.019	0.465	0.000	1.521
322	1,5-Anhydroglucitol	Sugars	0.003	0.002	0.233	0.004	1.733
7242	D-Allose	Sugars	0.247	0.372	−0.178	0.001	1.691
28,570	D-Mannose	Sugars	0.823	0.624	0.120	0.024	1.454
23,523	D-Mannose 1-phosphate	Sugars	0.046	0.024	0.279	0.017	1.517
342	D-Talose	Sugars	0.387	0.277	0.145	0.015	1.701
10,320	Stachyose	Sugars	0.017	0.030	−0.241	0.002	1.781
12,327	UDP-D-Galactose	Sugars	0.038	0.025	0.181	0.001	1.865
4690	UDP-N-acetylglucosamine	Sugars	0.013	0.009	0.141	0.003	1.659
13,544	UDP-D-Glucose	Sugars	0.088	0.055	0.209	0.001	1.855
122	Glycerol	Sugar alcohols	0.147	0.081	0.259	0.000	2.453
20,565	Glycerol	Sugar alcohols	0.061	0.034	0.254	0.020	1.560
233	3-Hydroxypropionic acid	Organic acids	0.038	0.021	0.257	0.018	1.676
55	Glycolic acid	Organic acids	0.003	0.002	0.145	0.025	1.356
8050	L-Malic acid	Organic acids	7.198	9.055	−0.100	0.008	1.568
24,217	Succinic acid	Organic acids	0.601	0.394	0.184	0.000	2.224
3290	D-Proline	Amino acids	0.104	0.083	0.096	0.004	1.559
215	Gamma-Aminobutyric acid	Amino acids	0.042	0.022	0.292	0.002	1.787
272	Betaine	Amines	1.151	1.583	−0.138	0.032	1.232
125	Ethanolamine	Amines	0.094	0.070	0.126	0.016	1.573
45	2-Hydroxypyridine	Pyridines	0.198	0.144	0.139	0.036	1.299
14,619	4-Hydroxycinnamic acid	Phenylpropanoids	0.093	0.063	0.169	0.043	1.319
168	Anabasine	Alkaloids	0.004	0.003	0.118	0.037	1.368
94	Methyl Phosphate	others	0.005	0.003	0.181	0.032	1.461
124	Orthophosphate	others	0.475	0.168	0.452	0.000	2.634
16,519	Pyruvaldehyde	others	0.416	0.352	0.073	0.019	1.386

Discussion

Characteristic metabolites of *Q. variabilis* at the subtropical P-rich site

Our results identified, for the first time, the metabolites that characterized the metabolome of plants at such extreme P-rich sites in the subtropics, which are generally characterized by P-limiting soils. These metabolites, which contributed most to discriminating *Q. variabilis* at the P-rich and P-deficient sites (VIP > 1), primarily were sugars, organic acids, amino acids, orthophosphate, etc. (Table 2). Ecologically, these metabolites in the present study were the result of plant adaptations to local soil nutrient environments under long-term interactions between nutrient requirements and their supply in soils in subtropical areas.

Of the 25 metabolites identified, several might be particularly representative of the physiological metabolism of plants in subtropical biomes. Within plant cells,

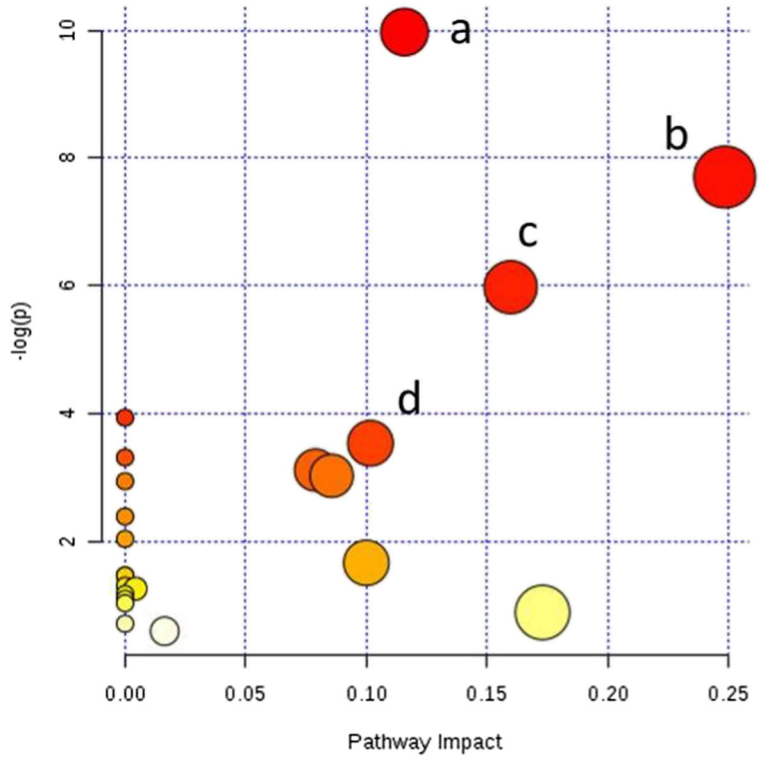

Fig. 3 Weight analysis of Metabolic pathways of *Q. variabilis* between P-rich site and P-deficient site. Each dot represents a metabolic pathway, there is positive correlation between the size/colour of the dots and metabolic pathways. **a**, Galactose metabolism; **b**, Amino sugar and nucleotide sugar metabolism; **c**, Glyoxylate and dicarboxylate metabolism; **d**, Fructose and mannose metabolism

P is a major component of nucleic acids, membrane lipids, and phsophorylated intermediates of energy metabolism. Thus, the cellular Pi homeostasis is essential for physiological and biochemical processes (Shen et al. 2011). In our study, orthophosphate was predominant in influencing the variation in the metabolome of *Q. variabilis* between the two P-type sites, possibly indicating its significance in maintaining physiological and biochemical processes of *Q. variabilis* in such P variable soils. Moreover, there was a significantly positive relationship, not only between the orthophosphate and leaf total P, but also between the leaf P and soil P at the P-rich site, suggesting the significance of orthophosphate in linking the metabolomes and ionomes of plants. Several studies have observed that the N:P ratio of foliage correlates negatively with plant growth (Elser et al. 2010) and biomass production (Güsewell 2004). In this study, leaf N:P correlated negatively with orthophosphate both at P-rich and P-deficient sites (Table S6), likely indicating importance of Pi in the growth of *Q. variabilis* in such P variable soils. These findings suggested that geologically P-rich soil had significant impacts on the formation of the P-rich metabotype in *Q. variabilis* at the P-rich site, which made the P-rich metabotype significantly different from the P-deficient metabotype in terms of metabolome.

The amino sugar and nucleotide sugar metabolic pathway, in which sugar metabolites (e.g., D-mannose, D-mannose-1-phosphate, and UDP-N-acetylglucosamine) were involved, was most affected likely due to the increasing supply of P in the soil at the P-rich site. Further, the three sugar metabolites involved in this pathway were significantly related to leaf P only at the P-rich site, which indicated that the *Q. variabilis* trees at the two P-type sites might have developed dissimilar metabolic strategies in adapting to local variation in P. Moreover, these strategies might involve the uptake and assimilation of P and modifications in carbon metabolism that bypass P-requiring steps (Gan et al. 2015; Plaxton and Carswell 1999; Uhde-Stone et al. 2003; Vance et al. 2003).

A number of nitrogen-containing compounds, including betaine, γ-Aminobutyric acid, D-proline, and UDP-N-acetyl-glucosamine, were related to leaf N at both the P-rich and P-deficient sites. Multiple studies have indicated that plants accumulated nitrogen-containing compounds, such as betaine, γ-Aminobutyric acid, and proline, primarily as osmolytes, in response to drought or salt stresses (Ashraf and

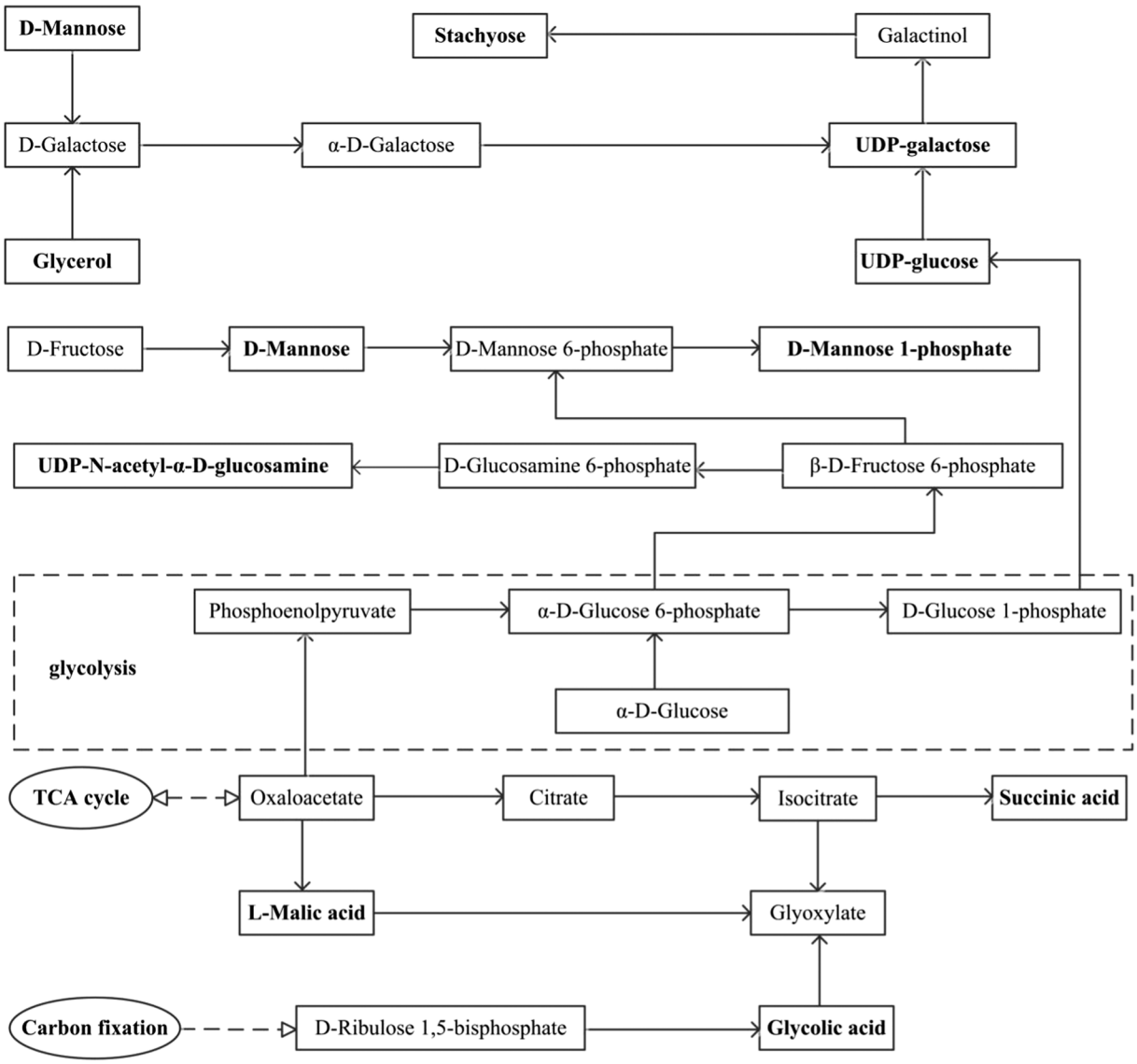

Fig. 4 Schematic diagram of the metabolic pathways. Metabolites in bold are potential biomarkers between P-rich and P-deficient sites. The most relevant pathways include: galactose metabolism, amino sugar and nucleotide sugar metabolism, glyoxylate and dicarboxylate metabolism, fructose and mannose metabolism

Foolad 2007; Carillo et al. 2008; Di Martino et al. 2003; Sawai et al. 2001; Serraj et al. 1998). Moreover, increasing nitrogen supplies had no effect on, or even decreased, the concentration of betaine; however, proline accumulation was more nitrogen-dependent (Carillo et al. 2008; Grattan and Grieve 1985; Monreal et al. 2007; Mulholland and Otte 2000; Mulholland and Otte 2002). Therefore, negative correlations between N and betaine, and positive correlations between N and proline and γ-Aminobutyric acid in *Q. variabilis* leaves may have a relationship in terms of stress tolerance in *Q. variabilis* tree populations.

Differential element-metabolite interactions at the P-rich and P-deficient sites

Our results indicated that the five elements (Zn, Fe, S, P, and N) and 25 discriminating metabolites not only contributed most to discriminating the two *Q. variabilis* populations between the P-rich and P-deficient sites (Table 2),

but also exhibited differential relationships between the two P-type sites. First, phosphorus-containing metabolites in *Q. variabilis* leaves seemed to be more closely related with P variation at the P-rich site in contrast to the P-deficient site. Second, there were significant correlations of leaf P with orthophosphate ($r = 0.85$, $p < 0.001$) and UDP-N-acetylglucosamine ($r = 0.80$, $p < 0.001$) at the P-rich site; however, the only correlation observed at the P-deficient site was that between total leaf P and orthophosphate ($r = 0.66$, $p < 0.01$). Third, leaf P was positively associated with the content of two other phosphorus-containing sugars (D-mannose-1-phosphate and UDP-N-acetylglucosamine) at the P-rich site, while no such relationship was observed at the P-deficient site. Fourth, the P content of the soil significantly affected the leaf P only at the P-rich site, but not at the P-deficient site (Figs. S4 and S5). All of these differences suggested that the relationships between elements and metabolites were altered at the P-rich site. Major causes might be that under long-term interactions between the physiological requirements of *Q. variabilis* and the supply of nutrients in the soils, their physiological and metabolic processes were characterized by the plentiful supply of mineral elements (N, P, Mg, S, etc.) in soils at the P-rich site (Yan et al. 2011; Zhu et al. 2015). Moreover, in contrast to general P-limiting sites in the subtropics, the weathering of phosphate rocks is a driving force for maintaining P and other minerals in soils at P-rich sites (Cernusak et al. 2010; Crews et al. 1995; Zhou et al. 2015).

Soil P-based ionomic and metabolomic phenotypes

Over the last five decades, intense efforts have been invested in the exploration of plant ecotype differentiation mechanisms on P-limiting soils (Silberbush et al. 1981; Snaydon and Bradshaw 1962; Xiao et al. 2009; Yan et al. 1995), and for the examination of P acquisition strategies under low P soil environments (Plaxton and Tran 2011; Sánchez-Calderón et al. 2010; Vance et al. 2003). The results of the present study, for the first time, revealed ionomic and metabolomic features for in situ trees at P-rich and P-deficient sites in subtropical areas. This might be related to plant adaptation mechanisms in response to variabilities in the P content of soils, and the formation of ecotypes.

Based on principal component analysis (PCA), the chemical composition of *Q. variabilis* leaves was significantly discriminated between the P-rich and P-deficient sites, in the formation of two distinct types of ionomes. For *Q. variabilis* population at the P-rich site, the ionome was characterized by elevated concentrations of seven elements (N, P, S, K, Mg, Fe, and Zn) (Table 1). Accordingly, there were significant differences in stoichiometry, and in particular, there were significantly lower leaf C:P, C:N, and N:P ratios at the P-rich site, compared with those at the P-deficient site (Table S7), which suggested adaptation-based interactions between plants and soils in terms of ecological stoichiometry (Cernusak et al. 2010; Reich and Oleksyn 2004). In addition, distinct leaf morphological traits were observed between *Q. variabilis* populations at the two P-type sites, with a larger specific leaf area ($cm^2\ g^{-1}$) at the P-rich site (Table S8). This highlights the differential leaf economics of *Q. variabilis* trees to the nutrient status of soils at P-rich and P-deficient sites (Wright et al. 2004). These results were consistent with other shrubs and grasses at different geological P sites (Ji et al. 2017; Tao 2005; Yan et al. 2011; Zhou et al. 2015). All of these data suggested that P-rich based soil phenotypic *Q. variabilis* populations existed in phosphate rock areas, which were interspersed with P-deficient ecosystems.

In our study, the PCA of GC-MS data was a less effective in discrimination of samples from the P-rich and P-deficient sites than the PCA of LC-MS data (Fig. 1b, c and d), as the used chromatographic platforms analyzed slightly different sets of metabolites and the GC-MS method differed from the LC-MS method by the relatively low repeatability of the analysis results. However, OPLS-DA analysis, that separated predictive variations (between groups) from nonpredictive variations (within groups) (Fonville et al. 2010), of GC-MS dataset showed good and significant discrimination of trees from P-rich and P-deficient sites. Moreover, PCA of all metabolite data obtained from LC-MS and GC-MS showed that the two *Q. variabilis* populations from P-rich and P-deficient sites were clearly separated (Fig. S3a). Thus and similarly, our study revealed that there was a distinct metabolome in the *Q. variabilis* population at the P-rich site, in contrast to that at the P-deficient site, where 25 metabolites contributed most to the variation in the metabolomes of the two *Q. variabilis* populations (Table 2). Of those 25 metabolites, most were phosphorus-containing (e.g., D-mannose 1-phosphate, UDP-D-galactose, UDP-D-glucose, UDP-N-acetylglucosamine, methylphosphate, and orthophosphate) and nitrogen-containing metabolites (e.g., UDP-D-galactose, UDP-D-glucose, UDP-N-

Table 3 Significant correlations (*r*, Pearson's correlation coefficient, *p* values in the parentheses) between the concentrations of N, P, S, Fe and Zn and content of the identified and discriminating metabolites obtained from the OPLS-DA analysis in the leaves of *Q. variabilis* trees growing at the P-rich and P-deficient sites. Significance, *p* value <0.05; *, negative relationships between the metabolite and the element

P-rich site	N	P	S	Fe	Zn	P-deficient site
D-Proline	0.60 (0.0224)					Betaine
Gamma-Aminobutyric acid	0.77 (0.0012)					D-Mannose
Succinic acid	0.77 (0.0013)*					D-Proline
D-Mannose		0.59 (0.0277)				Pyruvaldehyde
D-Mannose 1-phosphate		0.65 (0.0119)		0.61 (0.0195)*		UDP-N-acetylglucosamine
Orthophosphate		0.85 (0.0001)		0.62 (0.0169)*		Glycerol
UDP-N-acetylglucosamine		0.80 (0.0006)				Orthophosphate
Ethanolamine			0.56 (0.0386)	0.70 (0.0053)*		4-Hydroxycinnamic acid
L-Malic acid			0.59 (0.0250)*			1,5-Anhydroglucitol
4-Hydroxycinnamic acid				0.64 (0.0137)		Anabasine
Glycerol				0.59 (0.0265)*		D-Talose
2-Hydroxypyridine					0.54 (0.0445)	Glycolic acid
						Ethanolamine

P-rich site	N	P	S	Fe	Zn
D-Proline	0.70 (0.0049)*				
Gamma-Aminobutyric acid	0.67 (0.0126)				
Succinic acid	0.55 (0.0401)				
D-Mannose	0.57 (0.0440)				
D-Mannose 1-phosphate	0.65 (0.0153)*				
Orthophosphate		0.58 (0.0387)*			
UDP-N-acetylglucosamine		0.66 (0.0071)			
Ethanolamine			0.56 (0.0482)*		
L-Malic acid				0.52 (0.0472)*	
4-Hydroxycinnamic acid				0.60 (0.0191)*	
Glycerol				0.58 (0.0237)*	
2-Hydroxypyridine				0.54 (0.0392)*	
					0.52 (0.0451)

acetylglucosamine, D-proline, γ-Aminobutyric acid, betaine, ethanolamine, 2-Hydroxypyridine, and Anabasine). Some studies also found that P-deficiency reduced the content of phosphate and small phosphorylated metabolites (e.g., Glucose-6-P and Fructose-6-P) in plant leaf or root (Huang et al. 2008; Morcuende et al. 2007; Warren 2011). This highlights, to a certain extent, the characteristics of the phenotypic metabolome of *Q. variabilis* at P-rich sites. Moreover, these patterns were similar to the compositions of metabolites in plants under artificially controlled P starvation experiments (Gan et al. 2015).

Corresponding to differences in the leaf ionomes and metabolomes between the two P-type sites, the oak trees at the P-rich site exhibited significantly increased height and DBH in contrast to those at the P-deficient site (Fig. S6). Based on previous studies, plant stoichiometry (in particular, C:P and N:P ratios) reflect growth status, with a higher growth rate at lower C:P and N:P ratios in organisms (Matzek and Vitousek 2009; Sterner and Elser 2002; Yu et al. 2012). In this study, leaf N:P correlated negatively with UDP-N-acetylglucosamine, D-Mannose 1-phosphate and 4-Hydroxycinnamic acid (Table S6). This suggests that the compositions of metabolites also are closely associated with plant growth and development (Amtmann and Armengaud 2009; Balemi and Negisho 2012). For instance, artificially controlled experiments suggested that *Poplars* suppressed P/N uptake and assimilation during acclimation to P, N, or NP starvation at a P-deficient site (Gan et al. 2015). Moreover, many studies have shown that P deficiencies influenced carbohydrate metabolism in plants, and our results indicated that carbohydrate metabolism was likely upregulated in the P-rich *Q. variabilis* population compared to that in the P-deficient *Q. variabilis* population (Hernández et al. 2007; Morcuende et al. 2007; Nanamori et al. 2004; Vance et al. 2003). In our study, based on weight analysis, the 4 major pathways were all related to carbohydrate metabolism and 3 of which belong to sugar metabolism. Moreover, there was an overlap of metabolites involved in glyoxylate and dicarboxylate metabolism and TCA cycle (Fig. 4). Therefore, the four pathways, most likely to be differentially regulated in the leaves of the two *Q. variabilis* populations from the two P-type sites, would be important for the *Q. variabilis* to use sugars and obtain energy. Tawaraya et al. (2014) found that shoot P concentration and dry weight of soybean plants grown at P-deficient condition were lower than those at high P condition. Tissue et al. (2010) found that leaf P and carbohydrate of cottonwood seedlings increased with increasing P supply. Moreover, Xiao et al. (2009) found that the shoot biomass of the *Polygonum hydropiper* ecotype growing in a phosphorus mining area was ~2 fold higher than that of non-mining plant ecotype. Consistent with these studies, the ionome, metabolome, and growth in the present study indicated that there were likely two distinct ecotypes of *Q. variabilis* populations: a highly productive P-rich metabotype at P-rich sites, and a minimally productive P-deficient metabotype at P-deficient sites.

Conclusions

For this study, we characterized for the first time, the leaf ionome and metabolome of in situ trees at two contrasting P sites, which were derived from phosphate and non-phosphate rocks in subtropical biomes. Our results revealed that two *Q. variabilis* populations at P-rich and P-deficient sites had unique metabolomes and ionomes, which included five chemical elements (N, P, S, Fe, and Zn) and 25 metabolites (primarily as P- and N-containing compounds) that contributed most to the variation in the ionomes and metabolomes, respectively. Of these metabolites, orthophosphate was predominant in influencing the variation in the metabolomes of *Q. variabilis* between the two P-type sites, and furthermore, it displayed significantly positive relationships with leaf P, while leaf P was positively correlated with the soil P at the P-rich site, which demonstrated the potent effects of soil-enriched P on the variation in ionomes and metabolomes of the two *Q. variabilis* populations. Some pathways related to carbohydrate metabolism differed in the trees of the two *Q. variabilis* populations, which indicated that growth-related carbohydrate metabolism may be impacted by variation in geologic-P. These findings suggest that the two *Q. variabilis* populations growing at P-rich and P-deficient sites have formed differential metabolite and element compositions and correlations, and this may be related to the formation of the edaphic ecotypes and growth status adapted to the localized soil nutrient environments.

Acknowledgements This study was funded by the National Natural Science Foundation of China (No. 31670626, No. 31270640, and No. 31070532) and the National Key R&D Program of China (2017YFC0505501). We thank the Instrumental Analysis Center of Shanghai Jiao Tong University for the support on chemical analysis.

Data accessibility All data are included in the manuscript and the supplementary files, and all metabolites identified by GC-TOF-MS and UHPLC-QTOF-MS are included in the excel file named "ESM 2".

Authors' contributions C. Liu designed the study, H. Ji, B. Du and J. Wen collected field samples and data, H. Ji performed the experiments, and H. Ji, V. Ossipov and C. Liu analyzed the data and wrote the manuscript.

Compliance with ethical standards

Competing interests The authors declare no competing interests.

References

Amtmann A, Armengaud P (2009) Effects of N, P, K and S on metabolism: new knowledge gained from multi-level analysis. Curr Opin Plant Biol 12:275–283

Ashraf M, Foolad MR (2007) Roles of glycine betaine and proline in improving plant abiotic stress resistance. Environ Exp Bot 59:206–216

Attiwill PM, Adams MA (1993) Nutrient cycling in forests. New Phytol 124:561–582

Balemi T, Negisho K (2012) Management of soil phosphorus and plant adaptation mechanisms to phosphorus stress for sustainable crop production: a review. J Soil Sci Plant Nutr 12: 547–562

Brosché M, Vinocur B, Alatalo ER, Lamminmäki A, Teichmann T, Ottow EA, Djilianov D, Afif D, Bogeat-Triboulot M-B, Altman A (2005) Gene expression and metabolite profiling of *Populus euphratica* growing in the Negev desert. Genome Biol 6:R101

Carillo P, Mastrolonardo G, Nacca F, Parisi D, Verlotta A, Fuggi A (2008) Nitrogen metabolism in durum wheat under salinity: accumulation of proline and glycine betaine. Funct Plant Biol 35:412–426

Cernusak LA, Winter K, Turner BL (2010) Leaf nitrogen to phosphorus ratios of tropical trees: experimental assessment of physiological and environmental controls. New Phytol 185:770–779

Chen D, Zhang X, Kang H, Sun X, Yin S, Du H, Yamanaka N, Gapare W, Wu HX, Liu C (2012) Phylogeography of *Quercus variabilis* based on chloroplast DNA sequence in East Asia: multiple glacial refugia and mainland-migrated island populations. PLoS One 7:e47268

Cleveland CC, Townsend AR, Taylor P, Alvarez-Clare S, Bustamante M, Chuyong G, Dobrowski SZ, Grierson P, Harms KE, Houlton BZ (2011) Relationships among net primary productivity, nutrients and climate in tropical rain forest: a pan-tropical analysis. Ecol Lett 14:939–947

Crews TE, Kitayama K, Fownes JH, Riley RH, Herbert DA, Mueller-Dombois D, Vitousek PM (1995) Changes in soil phosphorus fractions and ecosystem dynamics across a long chronosequence in Hawaii. Ecology 76:1407–1424

Cronan CS, Grigal DF (1995) Use of calcium/aluminum ratios as indicators of stress in forest ecosystems. J Environ Qual 24: 209–226

Davey MP, Burrell MM, Woodward FI, Quick WP (2008) Population-specific metabolic phenotypes of *Arabidopsis lyrata* ssp. *petraea*. New Phytol 177:380–388

De Vos RCH, Moco S, Lommen A, Keurentjes JJB, Bino RJ, Hall RD (2007) Untargeted large-scale plant metabolomics using liquid chromatography coupled to mass spectrometry. Nat Protoc 2:778–791

Di Martino C, Delfine S, Pizzuto R, Loreto F, Fuggi A (2003) Free amino acids and glycine betaine in leaf osmoregulation of spinach responding to increasing salt stress. New Phytol 158: 455–463

Elser JJ, Fagan WF, Kerkhoff AJ, Swenson NG, Enquist BJ (2010) Biological stoichiometry of plant production: metabolism, scaling and ecological response to global change. New Phytol 186:593–608

FAO I (1998) World reference base for soil resources. World soil resources reports

Fester T, Merbach I, Schulz E, Härtig C (2014) Metabolic response of *Medicago sativa* to severe nutrient imbalances and disturbances under field conditions. J Plant Nutr Soil Sci 177:245–259

Fonville JM, Richards SE, Barton RH, Boulange CL, Ebbels TMD, Nicholson JK, Holmes E, Dumas M-E (2010) The evolution of partial least squares models and related chemometric approaches in metabonomics and metabolic phenotyping. J Chemom 24:636–649

Gan H, Jiao Y, Jia J, Wang X, Li H, Shi W, Peng C, Polle A, Luo Z (2015) Phosphorus and nitrogen physiology of two contrasting poplar genotypes when exposed to phosphorus and/or nitrogen starvation. Tree Physiol 36:22–38

Grattan SR, Grieve CM (1985) Betaine status in wheat in relation to nitrogen stress and to transient salinity stress. Plant Soil 85: 3–9

Guo R, Shi L, Yang C, Yan C, Zhong X, Liu Q, Xia X, Li H (2016) Comparison of ionomic and metabolites response under alkali stress in old and young leaves of cotton (*Gossypium hirsutum* L.) seedlings. Front. Plant Sci 7:1785

Güsewell S (2004) N: P ratios in terrestrial plants: variation and functional significance. New Phytol 164:243–266

Han W, Fang J, Guo D, Zhang Y (2005) Leaf nitrogen and phosphorus stoichiometry across 753 terrestrial plant species in China. New Phytol 168:377–385

Hänsch R, Mendel RR (2009) Physiological functions of mineral micronutrients (cu, Zn, Mn, Fe, Ni, Mo, B, cl). Curr Opin Plant Biol 12:259–266

Hernández G, Ramírez M, Valdés-López O, Tesfaye M, Graham MA, Czechowski T, Schlereth A, Wandrey M, Erban A, Cheung F (2007) Phosphorus stress in common bean: root transcript and metabolic responses. Plant Physiol 144:752–767

Huang CY, Roessner U, Eickmeier I, Genc Y, Callahan DL, Shirley N, Langridge P, Bacic A (2008) Metabolite profiling reveals distinct changes in carbon and nitrogen metabolism in phosphate-deficient barley plants (*Hordeum vulgare* L.). Plant Cell Physiol 49:691–703

Irakli L, Elser JJ (2011) The origins of the Redfield nitrogen-to-phosphorus ratio are in a homoeostatic protein-to-rRNA ratio. Ecol Lett 14:244–250

Ji H, Du B, Liu C (2017) Elemental stoichiometry and compositions of weevil larvae and two acorn hosts under natural phosphorus variation. Sci Rep 7:45810

Kawecki TJ, Ebert D (2004) Conceptual issues in local adaptation. Ecol Lett 7:1225–1241

Kimmins JP (2004) Forest ecology. Benjamin-Cummings Publishing Company, Menlo Park, California

Kind T, Wohlgemuth G, Lee DY, Lu Y, Palazoglu M, Shahbaz S, Fiehn O (2009) FiehnLib: mass spectral and retention index libraries for metabolomics based on quadrupole and time-of-flight gas chromatography/mass spectrometry. Anal Chem 81:10038–10048

Koerselman W, Meuleman AFM (1996) The vegetation N:P ratio: a new tool to detect the nature of nutrient limitation. J Appl Ecol 33:1441–1450

Lisec J, Schauer N, Kopka J, Willmitzer L, Fernie AR (2006) Gas chromatography mass spectrometry–based metabolite profiling in plants. Nat Protoc 1:387–396

Lundstedt T, Seifert E, Abramo L, Thelin B, Nyström Å, Pettersen J, Bergman R (1998) Experimental design and optimization. Chemom Intell Lab Syst 42:3–40

Matzek V, Vitousek PM (2009) N: P stoichiometry and protein: RNA ratios in vascular plants: an evaluation of the growth-rate hypothesis. Ecol Lett 12:765–771

Monreal JA, Jimenez ET, Remesal E, Morillo-Velarde R, García-Mauriño S, Echevarría C (2007) Proline content of sugar beet storage roots: response to water deficit and nitrogen fertilization at field conditions. Environ Exp Bot 60:257–267

Morcuende R, Bari R, Gibon Y, Zheng W, Pant BD, BLÄSING O, Usadel B, Czechowski T, Udvardi MK, Stitt M (2007) Genome-wide reprogramming of metabolism and regulatory networks of *Arabidopsis* in response to phosphorus. Plant Cell Environ 30:85–112

Mulholland MM, Otte ML (2000) Effects of varying sulphate and nitrogen supply on DMSP and glycine betaine levels in Spartina anglica. J Sea Res 43:199–207

Mulholland MM, Otte ML (2002) The effects of nitrogen supply and salinity on DMSP, glycine betaine and proline concentrations in leaves of Spartina anglica. Aquat Bot 72:193–200

Nanamori M, Shinano T, Wasaki J, Yamamura T, Rao IM, Osaki M (2004) Low phosphorus tolerance mechanisms: phosphorus recycling and photosynthate partitioning in the tropical forage grass, *Brachiaria hybrid* cultivar *Mulato* compared with rice. Plant Cell Physiol 45:460–469

Plaxton WC, Carswell MC (1999) Metabolic aspects of the phosphate starvation response in plants. In: Lerner HR (ed) Plant responses to environmental stresses: from phytohormones to genome reorganization. Marcel Dekker, Inc., New York, pp 349–372

Plaxton WC, Tran HT (2011) Metabolic adaptations of phosphate-starved plants. Plant Physiol 156:1006–1015

Raghothama KG (1999) Phosphate acquisition. Annu Rev Plant Biol 50:665–693

Reich PB, Oleksyn J (2004) Global patterns of plant leaf N and P in relation to temperature and latitude. Proc Natl Acad Sci U S A 101:11001–11006

Ribeiro DM, Silva Júnior DD, Cardoso FB, Martins AO, Silva WA, Nascimento VL, Araújo WL (2016) Growth inhibition by selenium is associated with changes in primary metabolism and nutrient levels in *Arabidopsis thaliana*. Plant Cell Environ 39:2235–2246

Rivas-Ubach A, Sardans J, Pérez-Trujillo M, Estiarte M, Peñuelas J (2012) Strong relationship between elemental stoichiometry and metabolome in plants. Proc Natl Acad Sci U S A 109: 4181–4186

Sanchez DH, Pieckenstain FL, Escaray F, Erban A, Kraemer U, Udvardi MK, Kopka J (2011) Comparative ionomics and metabolomics in extremophile and glycophytic *Lotus* species under salt stress challenge the metabolic pre-adaptation hypothesis. Plant Cell Environ 34:605–617

Sánchez-Calderón L, Chacon-López A, Pérez-Torres CA, Herrera-Estrella L (2010) Phosphorus: plant strategies to cope with its scarcity. In: Hell R, Mendel RR (eds) Cell biology of metals and nutrients. Springer, Berlin, Heidelberg, pp 173–198

Sardans J, Peñuelas J, Rivas-Ubach A (2011a) Ecological metabolomics: overview of current developments and future challenges. Chemoecology 21:191–225

Sardans J, Rivas-Ubach A, Peñuelas J (2011b) Factors affecting nutrient concentration and stoichiometry of forest trees in Catalonia (NE Spain). For Ecol Manage 262:2024–2034

Savolainen O, Pyhäjärvi T, Knürr T (2007) Gene flow and local adaptation in trees. Annu Rev Ecol Evol Syst 38:595–619

Sawai Y, Yamaguchi Y, Miyama D, Yoshitomi H (2001) Cycling treatment of anaerobic and aerobic incubation increases the content of γ-aminobutyric acid in tea shoots. Amino Acids 20:331–334

Schachtman DP, Reid RJ, Ayling SM (1998) Phosphorus uptake by plants: from soil to cell. Plant Physiol 116:447–453

Serraj R, Shelp BJ, Sinclair TR (1998) Accumulation of γ-aminobutyric acid in nodulated soybean in response to drought stress. Physiol Plant 102:79–86

Shaver GR, Chapin FSI, Billings WD (1979) Ecotypic differentiation in *Carex aquatilis* on ice-wedge polygons in the Alaskan coastal tundra. J Ecol 67:1025–1045

Shen J, Yuan L, Zhang J, Li H, Bai Z, Chen X, Zhang W, Zhang F (2011) Phosphorus dynamics: from soil to plant. Plant Physiol 156:997–1005

Shi C, Han R, Wu P, Fang M, Lai H, Shentu L (2011) Geochemistry and provenance of source rock for matoushan formation rocks (late cretaceous) in the Mouding area, Central Yunnan. Acta Sedimentol Sin 29:303–311

Silberbush M, Waisel Y, Kafkafi U (1981) The role of soil phosphorus in differentiation of edaphic ecotypes in *Aegilops peregrina*. Oecologia 49:419–424

Smith CA, Want EJ, O'Maille G, Abagyan R, Siuzdak G (2006) XCMS: processing mass spectrometry data for metabolite profiling using nonlinear peak alignment, matching, and identification. Anal Chem 78:779–787

Snaydon RW, Bradshaw AD (1962) Differences between natural populations of *Trifolium repens* L. in response to mineral nutrients. J Exp Bot 13:422–434

Soetan KO, Olaiya CO, Oyewole OE (2010) The importance of mineral elements for humans, domestic animals and plants: a review. Afr J Food Sci 4:200–222

Sterner RW, Elser JJ (2002) Ecological stoichiometry: the biology of elements from molecules to the biosphere. Princeton University Press, Princeton, NJ

Sun X, Kang H, Du H, Hu H, Zhou J, Hou J, Zhou X, Liu C (2012) Stoichiometric traits of oriental oak (*Quercus variabilis*) acorns and their variations in relation to environmental variables across temperate to subtropical China. Ecol Res 27: 765–773

Tao Y (2005) A proximate mathematical model of the content of main chemical constituents in an industrial phosphorus ore. Yunnan Geol 24:151–166

Tawaraya K, Horie R, Shinano T, Wagatsuma T, Saito K, Oikawa A (2014) Metabolite profiling of soybean root exudates under phosphorus deficiency. Soil Sci Plant Nutr 60:679–694

Tiessen H (2008) Phosphorus in the global environment. In: White PJ, Hammond JP (eds) The ecophysiology of plant-phosphorus interactions. Springer, Dordrecht, pp 1–7

Tillberg JE, Rowley JR (1989) Physiological and structural effects of phosphorus starvation on the unicellular green alga *Scenedesmus*. Physiol Plant 75:315–324

Tissue DT, Lewis JD, Niinemets Ü (2010) Photosynthetic responses of cottonwood seedlings grown in glacial through future atmospheric [CO2] vary with phosphorus supply. Tree Physiol 30:1361–1372

Uhde-Stone C, Zinn KE, Ramirez-Yáñez M, Li A, Vance CP, Allan DL (2003) Nylon filter arrays reveal differential gene expression in proteoid roots of white lupin in response to phosphorus deficiency. Plant Physiol 131:1064–1079

Vance CP, Uhde-Stone C, Allan DL (2003) Phosphorus acquisition and use: critical adaptations by plants for securing a nonrenewable resource. New Phytol 157:423–447

Vitousek P (1982) Nutrient cycling and nutrient use efficiency. Am Nat 119:553–572

Vitousek PM, Porder S, Houlton BZ, Chadwick OA (2010) Terrestrial phosphorus limitation: mechanisms, implications, and nitrogen-phosphorus interactions. Ecol Appl 20:5–15

Walker TW, Syers JK (1976) The fate of phosphorus during pedogenesis. Geoderma 15:1–19

Warren CR (2011) How does P affect photosynthesis and metabolite profiles of *Eucalyptus globulus*? Tree Physiol 31:727–739

Westheimer FH (1987) Why nature chose phosphates. Science 235:1173–1178

Wright IJ, Reich PB, Westoby M, Ackerly DD, Baruch Z, Bongers F, Cavender-Bares J, Chapin T, Cornelissen JH, Diemer M (2004) The worldwide leaf economics spectrum. Nature 428: 821–827

Wu Z, Zhu Y, Jiang H (1987) The vegetation of Yunnan. Science, Beijing

Wu D, Shen Q, Cai S, Chen Z, Dai F, Zhang G (2013) Ionomic responses and correlations between elements and metabolites under salt stress in wild and cultivated barley. Plant Cell Physiol 54:1976–1988

Xia J, Wishart DS (2010) MSEA: a web-based tool to identify biologically meaningful patterns in quantitative metabolomic data. Nucleic Acids Res 38:W71–W77

Xia J, Sinelnikov IV, Han B, Wishart DS (2015) MetaboAnalyst 3.0—making metabolomics more meaningful. Nucleic Acids Res 43:W251–W257

Xiao G, Li T, Zhang X, Yu H, Huang H, Gupta DK (2009) Uptake and accumulation of phosphorus by dominant plant species growing in a phosphorus mining area. J Hazard Mater 171: 542–550

Yan X, Lynch JP, Beebe SE (1995) Genetic variation for phosphorus efficiency of common bean in contrasting soil types: I. Vegetative response. Crop Sci 35:1086–1093

Yan K, Fu D, He F, Duan C (2011) Leaf nutrient stoichiometry of plants in the phosphorus-enriched soils of the Lake Dianchi watershed, southwestern China. Chin J Plant Ecol 35:353–361

Yan K, Ranjitkar S, Zhai D, Li Y, Xu J, Li B, Lu Y (2017) Current re-vegetation patterns and restoration issues in degraded geological phosphorus-rich mountain areas: a synthetic analysis of Central Yunnan, SW China. Plant Diversity 39:140–148

Yu Q, Wu H, He N, Lü X, Wang Z, Elser JJ, Wu J, Han X (2012) Testing the growth rate hypothesis in vascular plants with above-and below-ground biomass. PLoS One 7:e32162

Zhou X, Sun X, Du B, Yin S, Liu C (2015) Multielement stoichiometry in *Quercus variabilis* under natural phosphorus variation in subtropical China. Sci Rep 5:7839

Zhu F, Lu X, Liu L, Mo J (2015) Phosphate addition enhanced soil inorganic nutrients to a large extent in three tropical forests. Sci Rep 5:7923